CALCIOARAVAIPAITE
A NEW MINERAL
AND
ASSOCIATED LEAD FLUORIDE MINERALS FROM THE GRAND REEF MINE, GRAHAM COUNTY, ARIZONA

Anthony R. Kampf
Mineralogy Section
Natural History Museum of Los Angeles County
900 Exposition Blvd.
Los Angeles, California 90007

Eugene E. Foord
United States Geological Survey
Box 25046, Denver Federal Center, MS 905
Lakewood, Colorado 80225

The Grand Reef mine in southeastern Arizona, best known to collectors for superb crystals of linarite, is also the type locality for a unique suite of lead fluoride minerals. Grandreefite, pseudograndreefite, laurelite, aravaipaite, and artroeite have been found nowhere else; added to this group is calcioaravaipaite, described here for the first time.

INTRODUCTION

The Grand Reef mine is situated in Laurel Canyon, about 6 km northeast of Klondyke, in the Aravaipa mining district of Graham County, Arizona. Jones (1980) provided an overview of the history, geology and mineralogy of the deposit. The mineralogy was treated in greater detail in a thesis by Besse (1981). The mine exploits a small epithermal lead-copper-silver deposit hosted by a silicified breccia. The breccia is highly resistant to weathering and forms a precipitous cliff known as the "reef," from which the name of the mine is derived.

In 1969 a bench was blasted near the top of the reef just south of a vertical stope known as the "glory hole." Most of the mine's well-crystallized oxidized minerals, predominantly sulfates, have been recovered from this area. The fine linarite crystals up to 5 cm in length for which the mine is most famous were found here. This is also the source of six new lead fluoride minerals (Table 1). The first four, *grandreefite, pseudograndreefite, laurelite* and *aravaipaite,* were discovered on a single specimen (LACMNH 25414) recovered in 1980 during mining by Southwestern Mineral Associates

Figure 1. **The Grand Reef mine as viewed from the approach in Laurel Canyon. The new minerals were found near the "glory hole" opening about halfway up the face of the "reef" (center).**

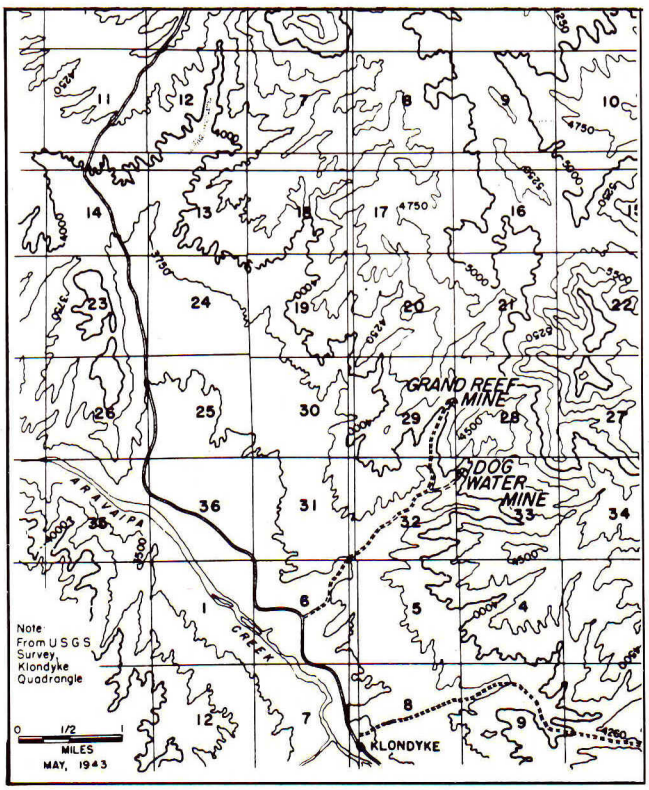

Figure 2. **Location map.**

***Table 1.* New lead fluoride minerals from the Grand Reef mine.**

Mineral	*Formula*
Grandreefite	$Pb_2F_2SO_4$
Pseudograndreefite	$Pb_6F_{10}SO_4$
Laurelite	$Pb_7F_{12}Cl_2$
Aravaipaite	$Pb_3Al(F,OH)_9$
Calcioaravaipaite	$PbCa_2Al(F,OH)_9$
Artroeite	$PbAlF_3(OH)_2$

(Richard Bideaux and Wayne Thompson). Two more, *artroeite* and *calcioaravaipaite*, were discovered on a specimen (LACMNH 39338) found in 1981 by Michael Shannon. The latter species is described for the first time in this study.

CALCIOARAVAIPAITE

Name and Deposition

Calcioaravaipaite is named for its relationship to aravaipaite; data imply that two of the three Pb atoms in aravaipaite are replaced by Ca atoms in calcioaravaipaite. The species and its name were approved by the Commission on New Minerals and Mineral Names, IMA, prior to publication. The type specimen has been deposited at the Natural History Museum of Los Angeles County.

Figure 3. **A portion of the type specimen of artroeite and calcioaravaipaite (LACMNH 39338). The white material in the vug is massive calcioaravaipaite covered with crystals of artroeite and calcioaravaipaite. Quartz layers with embedded fluorite surround the vug. The glassy, gray embedded crystal at the left is fluorite. The dark masses are galena partially altered to anglesite. The field of view is 1.5 cm across.**

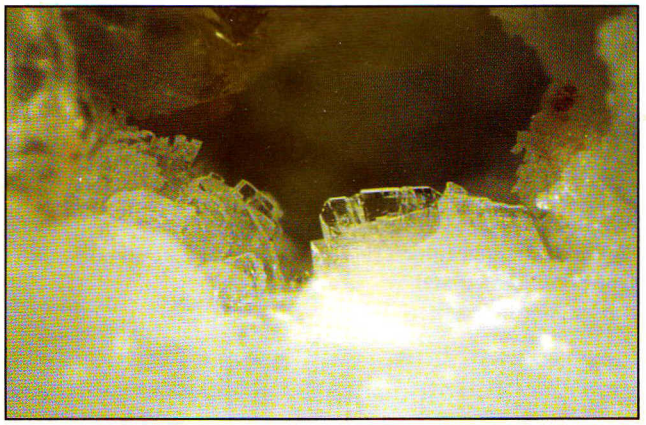

Figure 4. **Calcioaravaipaite (lower left) and artroeite crystals (lower center) on the type specimen (LACMNH 39338). The field of view is 2.5 mm across.**

Occurrence

Calcioaravaipaite is found on a single specimen in a 5 x 15-mm quartz-lined vug in association with crystals of anglesite and artroeite (Figures 1 and 2). Layers of quartz with embedded crystals of fluorite completely surround the vug. Crystals and masses of galena partially altered to anglesite form a discontinuous envelope bordering and included within the quartz layers. Linarite and muscovite are present outside of the galena envelope.

X-ray Crystallography

X-ray powder diffraction data, including calculated *d* values, are given in Table 2. Precession single-crystal studies, employing Zr-filtered Mo radiation, showed that calcioaravaipaite is monoclinic with space group *A*2, *A*2/*m*, or *Am*. The refined cell parameters based upon all powder reflections except the broad ones at 1.593 and 1.451 Å are provided in Table 3. Also presented in this table are parameters for an alternate cell of triclinic geometry compared to data for the triclinic cell of aravaipaite.

Precession films of aravaipaite and calcioaravaipaite are so similar, both in reflection patterns and intensities, that a close structural relationship between these minerals appears to be a virtual certainty. The triclinic cell of calcioaravaipaite is appreciably smaller than the equivalent cell of aravaipaite, as is to be expected when Ca takes the place of two-thirds of the Pb. Note that the triclinic cell parameters *a* and *c* and the angle β between them for aravaipaite and calcioaravaipaite compare closely to parameters of planes in the cubic fluorite structure-type of β-PbF_2 (*a* = 5.940 Å) and CaF_2 (*a* = 5.463 Å), respectively. This suggests that these structures may consist of (Pb,Ca)F_2 layers parallel to {010}, with Al–(F,OH) octahedra between layers. Unfortunately, crystals of both aravaipaite and calcioaravaipaite provide broad multiple reflections and are inadequate for structure determination.

Physical Characteristics

Calcioaravaipaite crystals were measured on a two-circle optical goniometer. They are tabular elongate on [011], flattened on {100}, and exhibit the forms {100} and {011}. (If the space group is *A*2, the form {$0\bar{1}1$} is also present; if the space group is *Am*, the forms {$\bar{1}00$} and {$0\bar{1}1$} are also present.) Twinning on {100} is ubiquitous. An orthographic projection of an idealized twinned crystal is shown in Figure 3. Maximum crystal dimensions are 0.05 x 0.3 x 0.7 mm. Calcioaravaipaite also occurs as a dense massive substrate for later-formed crystals of calcioaravaipaite and artroeite, and as tabular inclusions in artroeite reaching 10 microns in length.

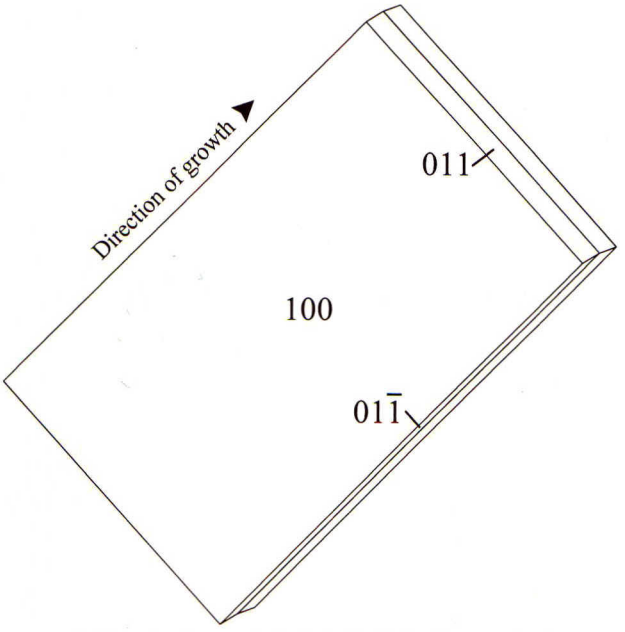

Figure 5. **Orthographic projection of a twinned crystal of calcioaravaipaite.**

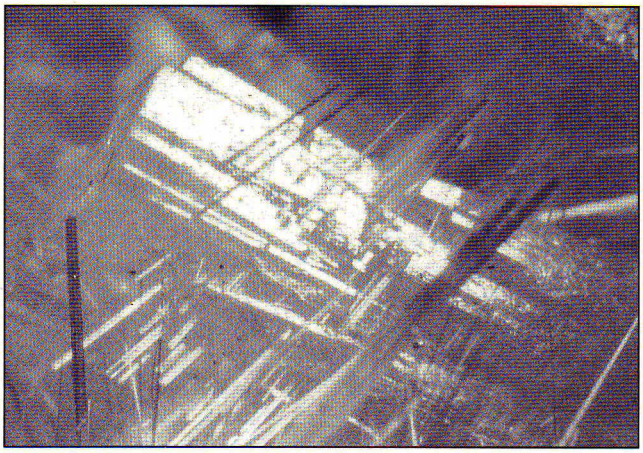

Figure 6. **Blocky crystal of pseudograndreefite with needles of laurelite on the type specimen of grandreefite, pseudograndreefite, laurelite and aravaipaite (LACMNH 25414). The field of view is 4 mm across.**

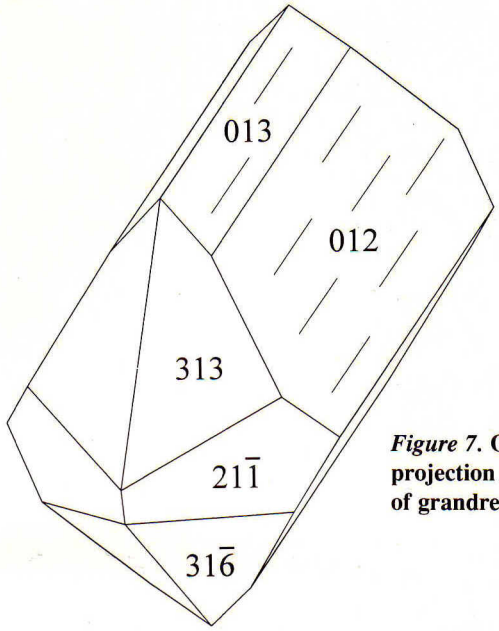

Figure 7. **Orthographic projection of a crystal of grandreefite.**

Crystals are colorless and transparent with a vitreous luster. The streak is white and the mineral is non-fluorescent. Crystals are brittle and possess a good {100} cleavage and conchoidal fracture. The Mohs hardness is about $2^1/_2$. The density determined by Berman balance on 2.4 mg is 4.85(5) g/cm^3. The calculated density assuming $Z = 8$ is 4.71 g/cm^3. Sample contamination with artroeite may be responsible for the higher measured density.

Optical Properties

The optical properties of calcioaravaipaite were determined by immersion using a Supper spindle stage. The mineral is optically biaxial (-). The indices of refraction measured in white light are $\alpha = 1.510(1)$, $\beta = 1.528(1)$, $\gamma = 1.531(1)$. The measured $2V$ is 36(2)°; the calculated $2V$ is 44°. Strong dispersion, $r > v$, was observed. The optical orientation is $Y = \mathbf{b}$, $Z \triangle \mathbf{c} = 73°$ in obtuse β.

Chemistry

Calcioaravaipaite was analyzed with an ARL-SEMQ electron microprobe at the U.S. Geological Survey in Denver, Colorado. The standards used were synthetic PbS, anhydrite, kyanite, and synthetic phlogopite for Pb, Ca, Al, and F, respectively. Water determination by moisture titration on 1.9 mg provided a value of 0.7 weight % H_2O. The accuracy of this value is questionable because of the very small sample size. The H_2O content obtained by difference (1.4 weight %) yields better stoichiometry and has therefore been used in the calculations below. The mean analytical results (and ranges) for five analyses are PbO = 46.4 (45.7–47.0), CaO = 23.5 (23.3–23.7), Al_2O_3 = 10.8 (10.7–10.9), F = 30.9 (30.8–31.1), H_2O = 1.4, sum 113.0, less O ≡ F 13.0, total 100.0 weight %.

The empirical formula based on 9 anions is $Pb_{1.02}Ca_{2.05}Al_{1.04}[F_{7.97}(OH)_{0.76}O_{0.27}]_{\Sigma 9.00}$. The simplified formula is $\mathbf{PbCa_2Al(F,OH)_9}$, which with F:OH = 8.1 requires PbO = 46.17, CaO = 23.21, Al_2O_3 = 10.55, F = 31.45, H_2O = 1.86, sum 113.24, less O ≡ F 13.24, total 100.00 weight %. The mineral dissolves slowly in H_2O and 1:1 HCl.

BRIEF DESCRIPTIONS of the OTHER NEW LEAD FLUORIDES

Grandreefite $Pb_2F_2SO_4$

Grandreefite was originally determined (Kampf *et al.*, 1989) to have an orthorhombic cell. Subsequent atomic structure determination (Kampf, 1991) showed it to be monoclinic, space group $A2/a$, $a = 8.667(1)$, $b = 4.4419(6)$, $c = 14.242(2)$ Å, $\beta = 107.418(2)°$, $Z = 4$. It occurs as colorless prismatic crystals striated parallel to [100] (Figure 4). The luster is subadamantine. Grandreefite has a Mohs hardness of about $2^1/_2$. It has a measured density of 7.0(1) g/cm^3. It decomposes rapidly in cold H_2O. Grandreefite is optically biaxial (+) with a very small $2V$ and weak dispersion, $r > v$. The indices of refraction are $\alpha = 1.872(5)$, $\beta = 1.873(5)$, $\gamma = 1.897(5)$; orientation $X \approx \mathbf{a}$, $Y = \mathbf{b}$, $Z \triangle \mathbf{c} = 17°$. Grandreefite is similar in structure to $La_2O_2SO_4$, based on layer fragments of the β-PbF_2 (fluorite) structure parallel to (100) with SO_4 groups between layers.

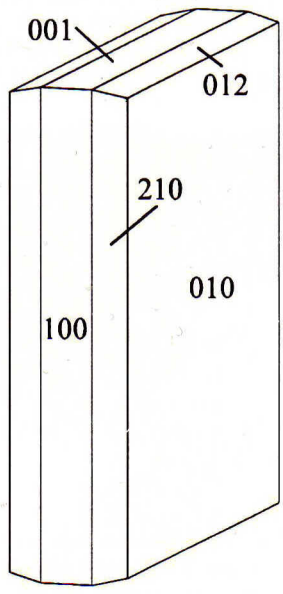

Figure 8. **Orthographic projection of a crystal of pseudograndreefite.**

Pseudograndreefite $Pb_6F_{10}SO_4$

Pseudograndreefite (Kampf *et al.*, 1989) is orthorhombic, space group $F222$, $a = 8.5182(5)$, $b = 19.5736(11)$, $c = 8.4926(5)$ Å, $Z = 4$. It occurs as colorless square crystals tabular on {010} (Figures 5 and 6). The luster is subadamantine. Pseudograndreefite has a Mohs hardness of about $2^1/_2$. It has a measured density of 7.0(1) g/cm^3. It decomposes rapidly in cold H_2O. Pseudograndreefite is

optically biaxial (+) with $2V = 30(3)°$ and strong dispersion, $r > v$. The indices of refraction are $\alpha = 1.864(5)$, $\beta = 1.865(5)$, $\gamma = 1.873(5)$; orientation X = **c**, Y = **a**, Z = **b**. The structure of pseudograndreefite has not been completely solved but is very similar to that of grandreefite, based on double layer fragments of the β-PbF_2 (fluorite) structure parallel to {010} with SO_4 groups between layers.

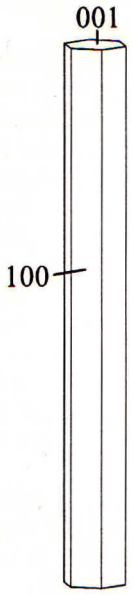

Figure 9. **Orthographic projection of a crystal of laurelite.**

Laurelite $Pb_7F_{12}Cl_2$

Laurelite (Kampf *et al.*, 1989) is hexagonal, space group $P\bar{6}$, a = 10.252(9), c = 3.973(1) Å, Z = 1. Most typically it occurs as thin tapering needles grouped into parallel bundles. Rarely it occurs as colorless simple hexagonal prisms (Figures 5 and 7). Broken surfaces across densely packed crystal bundles provide a subadamantine luster; the surfaces of crystal bundles have a silky luster. Laurelite has a Mohs hardness of about 2. The original measured density of 6.2(1) g/cm³ was obtained using a pycnometer and a sample consisting of many small difficult-to-handle needles. Subsequently, three large crystal fragments weighing a total of 13 mg provided a better density measurement of 7.65 g/cm³ on a Berman balance. Laurelite decomposes rapidly in cold 1:1 HCl and dissolves very slowly in cold H_2O. It is optically uniaxial (+), with $\omega = 1.903(5)$, $\varepsilon = 1.946(5)$. The structure of laurelite (report by S. Merlino, M. Pasero, N. Perchiazzi and A. Kampf submitted for publication) is closely related to that of α-PbF_2 consisting of layers of nine-coordinated Pb parallel to {001}.

Aravaipaite $Pb_3Al(F,OH)_9$

Aravaipaite (Kampf *et al.*, 1989) is triclinic, space group $P1$ or $P\bar{1}$, a = 5.842(2), b = 25.20(5), c = 5.652(2) Å, $\alpha = 93.84(4)$, $\beta = 90.14(4)$, $\gamma = 85.28(4)°$, Z = 4. It occurs as colorless, thin, flexible plates with perfect micaceous {010} cleavage (Fig. 8). Polysynthetic twinning on {010} is ubiquitous. The luster is vitreous to pearly. Aravaipaite has a Mohs hardness of about 2, and a calculated density of 6.37 g/cm³. Aravaipaite decomposes rapidly in cold 1:1 HCl and dissolves very slowly in cold H_2O. It is optically biaxial (-) with $2V = 70(3)°$ and strong dispersion, $r < v$. The indices of refraction are $\alpha = 1.678(2)$, $\beta = 1.690(2)$, $\gamma = 1.694(2)$; Euler angles are $\varphi = 67°$, $\psi = 60°$, $\theta = 76°$. As noted earlier, the structure of aravaipaite may be related to that of β-PbF_2 with layers of the β-PbF_2 structure parallel to {010} and Al–(F,OH) octahedra between layers.

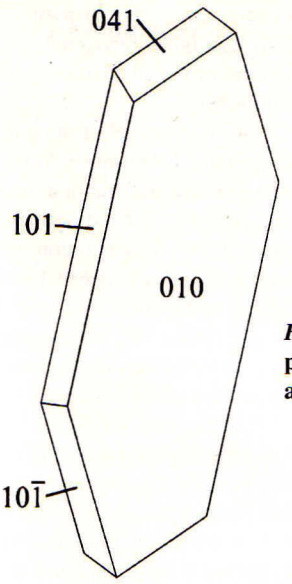

Figure 10. **Orthographic projection of a crystal of aravaipaite.**

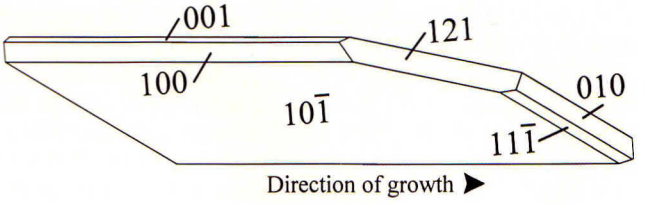

Figure 11. **Orthographic projection of a crystal of artroeite.**

Artroeite $PbAlF_3(OH)_2$

Artroeite (Kampf and Foord, 1995) is triclinic, space group $P\bar{1}$, a = 6.270(2), b = 6.821(3), c = 5.057(2) Å, $\alpha = 90.68(2)$, $\beta = 107.69(2)$, $\gamma = 104.46(2)°$, Z = 2. It occurs as colorless, bladed crystals (Figure 2 and 9) with perfect {100} cleavage and good {010} cleavage. The luster is vitreous. Artroeite has a Mohs hardness of about 2½. It has a measured density of 5.36(2) g/cm³. Artroeite is optically biaxial (-) with $2V = 41°$ and strong dispersion, $r > v$. The indices of refraction are $\alpha = 1.629(1)$, $\beta = 1.682(2)$, and $\gamma = 1.691(2)$. The structure of artroeite consists of edge-sharing dimers of $AlF_3(OH)_3$ octahedra linked together via bonds to Pb atoms to form approximately close-packed layers parallel to {10$\bar{1}$}.

PARAGENESIS of the LEAD FLUORIDES

Observations

It is known that the specimens containing the new lead fluoride minerals were all recovered from the bench area that has produced most of the other well-crystallized oxidized minerals at the mine. Unfortunately, the details of the recovery of these specimens, including their specific contexts in this assemblage, are not known. To date the most complete picture of the surrounding assemblage is provided by a reconstructed block of matrix measuring about 15 x 25 x 27 cm that originally abutted the type specimen containing grandreefite, pseudograndreefite, laurelite and aravaipaite

(LACMNH 25414). The type specimen containing artroeite and calcioaravaipaite (LACMNH 39338) and other recovered specimens containing these new minerals have provided additional clues to the paragenesis of these unique minerals.

The aforementioned reconstructed block is typical of the mineralization found in the bench area of the Grand Reef mine. Veins of galena follow irregular fractures in the breccia, and minor amounts of copper sulfides associated with the galena are altered principally to linarite and caledonite. The galena shows lesser alteration to anglesite. Galena veins often border interstices between breccia blocks, and the gangue minerals fluorite and quartz commonly fill these interstices. The vug containing grandreefite, pseudograndreefite, laurelite and aravaipaite occupies the center of an interstice between breccia blocks. Although a portion of the rock surrounding the vug is missing, it is clear that the vug was completely surrounded by galena. An irregular and incomplete layer of fluorite is found inside the galena layer, followed by a complete layer of quartz surrounding the quartz-lined vug. Anglesite fills narrow fractures in the quartz. A few centimeters away from this vug, another interstice in the breccia is bordered by galena and completely filled by massive fluorite.

The type specimen containing artroeite and calcioaravaipaite is similar in character. An intergrowth of fluorite and galena completely envelops the quartz-lined vug. The galena is partially altered to anglesite. The artroeite and calcioaravaipaite are associated with anglesite crystals within the vug. Linarite and muscovite are present outside of the fluorite/galena envelope.

Laurelite appears to be the most widespread of the new minerals. Numerous specimens containing laurelite were examined in the course of this study. In general the laurelite occurs in quartz-lined vugs that are surrounded by galena. The laurelite is usually found growing on or in close proximity to fluorite. In some instances the fluorite shows evidence of dissolution. Anglesite crystals are commonly associated with laurelite, the anglesite clearly preceding the crystallization of the laurelite. In only two instances was linarite found in close proximity to laurelite.

The evidence suggests the following order of crystallization: galena → fluorite → quartz → anglesite → lead fluorides. Among the lead fluorides the order of crystallization based upon the first type specimen (LACMNH 25414) is: grandreefite → pseudograndreefite → laurelite → aravaipaite; the order based upon the second type specimen (LACMNH 39338) is: calcioaravaipaite → artroeite. Intergrowth relationships between the lead fluorides indicate significant overlaps in their periods of crystallization.

The secondary calcium fluoride minerals gearksutite and creedite were reported from the mine by Jones (1980) and Besse (1981). Besse reported gearksutite to be moderately common in the bench area as a very late-stage, chalky cavity filling. Besse (personal communication, 1988) also reported the occurrence of prosopite in an isolated vug in the bench area. None of these minerals were observed in association with the new lead fluoride minerals, although small amounts of gearksutite are present in the matrix surrounding the first vug.

Cerussite is a common supergene alteration product of galena at the Grand Reef mine, although it is less common than anglesite in the surface exposure of the vein (Jones, 1980). Notably, cerussite was not found on any of the specimens bearing the new lead fluoride minerals.

Chemical Considerations

The presence of Pb^{2+} in solution is clearly critical to the formation of the new minerals. Because of the strong tendency of this ion to combine with SO_4^{2-} or CO_3^{2-}, its mobility in systems dominated by these anions is very limited (*cf.* Garrels and Christ, 1965). Close proximity of galena to a source of F^- is seemingly necessary for the formation of the new minerals.

Solution attack on fluorite, the obvious source of F^- in the system, would release Ca^{2+} as well. In this respect, the absence of the secondary calcium fluoride minerals gearksutite and creedite in the vugs with the new lead fluorides, and the presence of essential calcium in only one of the new lead fluorides, calcioaravaipaite, is notable. The Ca^{2+}, having a much greater mobility (solubility) than Pb^{2+} in solution in the presence of SO_4^{2-} and F^-, probably migrated away from the vicinity of the vug.

As evidenced by the abundance of supergene sulfate mineralization, acidic sulfate-rich solutions were apparently dominant during the formation of much of the secondary oxidized assemblage in the upper portion of the bench. The absence of cerussite on any of the specimens containing the lead fluoride minerals suggests at least a local dearth of CO_3^{2-} in the supergene solutions. Aside from the obvious requirement of SO_4^{2-} for the formation of grandreefite and pseudograndreefite (which contain essential SO_4^{2-}), the initial presence of SO_4^{2-} and absence of CO_3^{2-} in solution may also have been critical to the formation of all of the new lead fluoride minerals.

The selective incorporation of chloride in laurelite is probably attributable to the preference of chloride for the α-$PbF_2(PbCl_2)$ structural arrangement. The greater abundance of this mineral relative to the other new lead fluorides may also be related to its ability to accommodate chloride.

The aluminum essential to aravaipaite, calcioaravaipaite and artroeite was probably provided by the invading supergene solutions which had acquired the aluminum through reaction with silicates such as muscovite occurring in the breccia.

Interpretations

The new lead fluoride minerals are interpreted as resulting from the reaction of late-stage supergene solutions with galena and fluorite. This is suggested by the compositions of the new minerals, by their spatial proximity to galena and fluorite, by dissolution features noted in some fluorite, by alteration of the galena surrounding the vug, and by the formation of anglesite both as a fracture-filling in the quartz lining and as crystals in the vugs prior to the crystallization of the lead fluoride minerals.

The crystallization of anglesite before the lead fluorides and (in the first vug) the crystallization of grandreefite and pseudograndreefite before aravaipaite and laurelite, represent progressions from sulfate-rich to fluoride-rich phases. This is consistent with progressive crystallization under closed-system conditions within the vug and, together with the earlier presented evidence, suggests the following sequence of formation: (1) the incoming acidic sulfate-rich supergene solution reacts with galena and fluorite as it enters the open vug, (2) the F^- concentration of the solution trapped in the vug increases as SO_4^{2-} is preferentially incorporated into earlier crystallizing anglesite, (3) the new lead fluoride minerals form from the increasingly fluoride-rich solution, and (4) the galena-fluorite-quartz envelope around the vug isolates it from further interaction with aqueous solutions, thereby preserving the lead fluoride minerals.

Isolated vugs containing mineralization quite distinct from nearby vugs are typical of the Grand Reef mine (Wayne Thompson, personal communication, 1988). These may be attributed to the mode of emplacement of the orebody according to the following scenario. When the orebody was emplaced in the breccia, the interstices between breccia blocks were in-filled with layers of sulfides (mostly galena) and gangue minerals (mostly fluorite and quartz). During supergene alteration of the deposit, solutions entered the open vugs through fractures in the surrounding layers of galena, fluorite and quartz. Initial crystallization of supergene

***Table 2.* X-ray powder diffraction data for calcioaravaipaite.**

I/I_o	d_{obs}	d_{calc}	hkl_m	hkl_t
100	11.9	11.94	200	$0\bar{2}0$
10	5.22	5.214	111	$\bar{1}10$, 011
20	4.85	4.853	$2\bar{1}1$	$\bar{1}20$, $02\bar{1}$
5	4.51	4.514	$\bar{3}11$	$\bar{1}30$, $0\bar{3}1$
20	4.40	4.400	$3\bar{1}1$	$\bar{1}30$, $03\bar{1}$
5	4.06	4.051	$\bar{4}11$	$\bar{1}40$, $0\bar{4}1$
10	3.93	3.942	$4\bar{1}1$	$\bar{1}40$, $04\bar{1}$
35	3.82	3.821	$\bar{1}02$	$11\bar{1}$
70	3.71	3.712	$1\bar{2}0$	$\bar{1}11$, $1\bar{1}1$
5	3.62	3.621	$\bar{5}11$	$\bar{1}50$, $0\bar{5}1$
85	3.51	3.523	$5\bar{1}1$	$\bar{1}50$, $05\bar{1}$
		3.518	$\bar{3}02$	$13\bar{1}$
50	3.406	3.411	302	$\bar{1}31$
		3.399	$3\bar{2}0$	131, $1\bar{3}1$
20	3.235	3.242	$\bar{6}11$	$\bar{1}60$, $0\bar{6}1$
20	3.157	3.158	611	$\bar{1}60$, 061
60	2.981	2.986	800	$0\bar{8}0$
60	2.943	2.940	$50\bar{2}$	$\bar{1}51$
5	2.847	2.846	711	$\bar{1}70$, 071
50	2.692	2.688	$0\bar{2}2$	200, $00\bar{2}$
45	2.638	2.638	$\bar{2}22$	$2\bar{2}0$, $0\bar{2}2$
5	2.509	2.504	702	$\bar{1}71$
30	2.390	2.389	10·0·0	0·10·0
5	2.331	2.331	$2\bar{3}1$	$2\bar{2}1$, 122
15	2.274	2.278	$4\bar{1}3$	$24\bar{1}$, $14\bar{2}$
		2.275	331	132, $2\bar{3}1$
5	2.223	2.226	$90\bar{2}$	$19\bar{1}$
		2.220	$4\bar{1}3$	$\bar{1}42$, $\bar{2}41$
10	2.204	2.206	$\bar{10}$·1·1	1·10·0, 0·$\bar{10}$·1
		2.203	431	142, $24\bar{1}$
5	2.164	2.168	920	191, $199\bar{1}$
		2.161	10·1·1	$\bar{1}$·10·0, 0·10·1
5	2.144	2.145	$90\bar{2}$	$19\bar{1}$
5	2.109	2.107	$6\bar{1}3$	$26\bar{1}$, $16\bar{2}$
60	2.028	2.026	$\bar{8}22$	280, $08\bar{2}$
5	1.989	1.991	12·0·0	$0\bar{1}2$·0
60	1.971	1.971	$82\bar{2}$	$\bar{2}80$, 082
25	1.926	1.924	$\bar{11}$·0·2	1·$1\bar{1}$·$\bar{1}$
		1.923	004	$20\bar{2}$
50	1.879	1.879	040	$20\bar{2}$
5	1.852	1.852	$\bar{4}04$	$24\bar{2}$
10	1.790	1.792	$0\bar{3}3$	300, $00\bar{3}$
		1.791	$\bar{1}33$	310, $01\bar{3}$
5	1.758	1.759	$\bar{6}04$	$33\bar{0}$, $03\bar{3}$
		1.759	$\bar{3}33$	$26\bar{2}$
40	1.686	1.686	$\bar{1}42$	311, $11\bar{3}$
		1.686	$\bar{3}24$	133, $33\bar{1}$
15	1.657	1.657	$\bar{3}42$	331, $13\bar{3}$
5	1.651	1.651	$\bar{6}33$	360, $06\bar{3}$
10	1.622	1.621	$\bar{12}$·2·2	2·12·0, 0·$\bar{12}$·2
45b	1.593	1.595	11·3·1	$\bar{1}$·11·2, 2·$\bar{11}$·1
		1.594	$52\bar{4}$	$\bar{3}51$, $15\bar{3}$
		1.593	$62\bar{4}$	$36\bar{1}$, $16\bar{3}$
		1.590	840	$28\bar{2}$, $28\bar{2}$
		1.589	11·1·3	$\bar{1}$·11·2, 2·$\bar{11}$·1
5	1.557	1.556	$8\bar{3}3$	380, $08\bar{3}$
5	1.539	1.539	$\bar{15}$·1·1	1·15·0, 0·$\bar{15}$·1
15	1.520	1.518	12·3·1	1·12·2, 2·$\bar{12}$·1
10	1.493	1.493	16·0·0	$0\bar{1}6$·0
5	1.467	1.467	$93\bar{3}$	$\bar{3}90$, 093
5b	1.451	1.453	$\bar{10}$·3·3	3·10·0, 0·$\bar{10}$·3
		1.449	$\bar{16}$·1·1	1·16·0, 0·$\bar{16}$·1
5	1.414	1.415	10·3·3	$\bar{3}$·10·0, 0·10·3
10	1.369	1.369	$\bar{10}$·2·4	$\bar{3}$·10·1, $\bar{1}$·$\bar{10}$·3
		1.369	$\bar{17}$·1·1	1·17·0, 0·$\bar{17}$·1
10	1.344	1.344	$04\bar{4}$	400, 004
20	1.320	1.321	$\bar{16}$·2·2	2·16·0, 0·$\bar{16}$·2
		1.319	$\bar{4}44$	440, $04\bar{4}$

hkl_m: indices based upon monoclinic cell, a = 23.905(5), b = 7.516(2), c = 7.699(2) Å, β = 92.25(2)°.

hkl_t: indices based upon alternate cell with triclinic geometry, a = 5.380(1), b = 23.905(4), c = 5.380(1) Å, α = 91.62(2)°, β = 91.38(2)°, γ = 88.38(2)°.

114.6-mm Gandolfi camera; Ni-filtered Cu$K\alpha$ radiation; intensities visually estimated.

***Table 3.* Comparison of crystallographic data for aravaipaite and calcioaravaipaite.**

		Aravaipaite	*Calcioaravaipaite*	
Chemical formula		$Pb_3Al(F,OH)_9$	$PbCa_2Al(F,OH)_9$	
Crystal system		triclinic	triclinic§	monoclinic
Space group		$P1$ or $P\bar{1}$		$A2$, Am or $A2/m$
Cell parameters	a	5.842(2) Å	5.380(1) Å	23.906(5) Å
	b	25.20(5) Å	23.905(4) Å	7.516(2) Å
	c	5.652(2) Å	5.380(1) Å	7.699(2) Å
	α	93.84(4)°	91.62(2)°	
	β	90.14(4)°	91.38(2)°	92.25(2)°
	γ	85.28(4)°	88.38(2)°	
	V	827(2) Å^3	691.1(2) Å^3	1382.2(4) Å^3
	Z	4	4	8

* Aravaipaite cell data from Kampf *et al.*, 1989

§ Alternate cell with triclinic geometery.

minerals sealed the entrance fractures, thereby isolating the vugs from further interaction with supergene solutions and creating individual micro-environments within the vugs. Small local variations in chemistry were then accentuated by progressive crystallization under closed-system conditions. Another example of a unique micro-environment mineral occurrence at the Grand Reef mine is shannonite, Pb_2OCO_3, recently described by Roberts *et al.* (1995).

ACKNOWLEDGMENTS

We acknowledge contributions to this study by a number of individuals. William Besse brought the type specimen of grandreefite, pseudograndreefite, laurelite and aravaipaite to the attention of the senior author. Wayne Thompson and Richard A. Bideaux of *Southwestern Mineral Associates* donated this specimen. David Shannon of *David Shannon Minerals* donated the type specimen of artroeite and calcioaravaipaite. Les Presmyk and Renato Pagano made additional material available for examination. William Besse, Wayne Thompson and David Shannon provided information regarding the geology and mineralogy of the Grand

Reef mine. Larry L. Jackson of the U.S. Geological Survey in Denver conducted the moisture titration on calcioaravaipaite. Peter A. Williams of the University of Western Sydney Nepean, Australia, provided helpful comments regarding the paragenesis. The manuscript benefited from a review by Donald R. Peacor of the University of Michigan and suggestions by Dorothy Ettensohn of the Natural History Museum of Los Angeles County.

REFERENCES

BESSE, W. W. (1981) The mineralogy of the Grand Reef mine, Aravaipa mining district, Graham County, Arizona. M.S. thesis, Department of Geology, California State University at Los Angeles.

GARRELS, R. M., and CHRIST, C. L. (1965) *Solutions, Minerals, and Equilibria*. Harper and Row, New York, 450 p.

JONES, R. W. (1980) The Grand Reef mine, Graham County, Arizona. *Mineralogical Record*, **11**, 219–225.

KAMPF, A. R. (1991) Grandreefite, $Pb_2F_2SO_4$: crystal structure and relationship to the lanthanide oxide sulfates, $Ln_2O_2SO_4$. *American Mineralogist*, **76**, 278–282.

KAMPF, A. R., DUNN, P. J., and FOORD, E. E. (1989) Grandreefite, pseudograndreefite, laurelite, and aravaipaite: Four new minerals from the Grand Reef mine, Graham County, Arizona. *American Mineralogist*, **74**, 927–933.

KAMPF, A. R., and FOORD, E. E. (1995) Artroeite, $Pb\,AlF_3(OH)_2$, a new mineral from the Grand Reef mine, Graham County, Arizona: Description and crystal structure. *American Mineralogist*, **80**, 179–183.

MERLINO, S., PASERO, M., PERCHIAZZI, N., and KAMPF, A. R. (1996?) Laurelite: Its atomic structure and relationship to alpha-PbF_2. (manuscript submitted for publication)

ROBERTS, A. C., STIRLING, J. A. R., CARPENTER, G. J. C., CRIDDLE, A. J., JONES, G. C., BIRKETT, T. C., and BIRCH, W. D. (1995) Shannonite, Pb_2OCO_3, a new mineral from the Grand Reef mine, Graham County, Arizona, USA. *Mineralogical Magazine*, **59**, 305–310.